RADIATION RESEARCH **187**, 493–501 (2017)
0033-7587/17 $15.00

DOI: 10.1667/RR0010CC.1

Germicidal Efficacy and Mammalian Skin Safety of 222-nm UV Light

Manuela Buonanno,[a] Brian Ponnaiya,[a] David Welch,[a] Milda Stanislauskas,[b] Gerhard Randers-Pehrson,[a] Lubomir Smilenov,[a] Franklin D. Lowy,[c] David M. Owens[b,d] and David J. Brenner[a,1]

[a] *Center for Radiological Research, Departments of* [b] *Dermatology,* [c] *Medicine and Infectious Diseases,* [d] *Pathology and Cell Biology, Columbia University Medical Center, New York, New York*

Buonanno, M., Ponnaiya, B., Welch, D., Stanislauskas, M. Randers-Pehrson, G., Smilenov, L., Lowy, F. D., Owens, D. M. and Brenner, D. J. Germicidal Efficacy and Mammalian Skin Safety of 222-nm UV Light. *Radiat. Res.* 187, 493–501 (2017).

We have previously shown that 207-nm ultraviolet (UV) light has similar antimicrobial properties as typical germicidal UV light (254 nm), but without inducing mammalian skin damage. The biophysical rationale is based on the limited penetration distance of 207-nm light in biological samples (e.g. stratum corneum) compared with that of 254-nm light. Here we extended our previous studies to 222-nm light and tested the hypothesis that there exists a narrow wavelength window in the far-UVC region, from around 200–222 nm, which is significantly harmful to bacteria, but without damaging cells in tissues. We used a krypton-chlorine (Kr-Cl) excimer lamp that produces 222-nm UV light with a bandpass filter to remove the lower- and higher-wavelength components. Relative to respective controls, we measured: 1. *in vitro* killing of methicillin-resistant *Staphylococcus aureus* (MRSA) as a function of UV fluence; 2. yields of the main UV-associated premutagenic DNA lesions (cyclobutane pyrimidine dimers and 6-4 photoproducts) in a 3D human skin tissue model *in vitro*; 3. eight cellular and molecular skin damage endpoints in exposed hairless mice *in vivo*. Comparisons were made with results from a conventional 254-nm UV germicidal lamp used as positive control. We found that 222-nm light kills MRSA efficiently but, unlike conventional germicidal UV lamps (254 nm), it produces almost no premutagenic UV-associated DNA lesions in a 3D human skin model and it is not cytotoxic to exposed mammalian skin. As predicted by biophysical considerations and in agreement with our previous findings, far-UVC light in the range of 200–222 nm kills bacteria efficiently regardless of their drug-resistant proficiency, but without the skin damaging effects associated with conventional germicidal UV exposure. © 2017 by Radiation Research Society

INTRODUCTION

The use of ultraviolet (UV) light for inactivating bacteria and viruses is well established (*1, 2*). However, UV radiations emitted by typical germicidal lamps with a peak emission at 254 nm represent a human health hazard, causing skin cancer (*3, 4*) and cataracts (*5, 6*).

We have developed an approach to kill bacteria without harming human cells in skin tissue models (*7*) and mouse skin *in vivo* (*8*) that employs single-wavelength UVC light generated by inexpensive filtered excilamps (*9*). The approach is based on the limited penetration distance of UVC light in the wavelength range of 200–222 nm in biological samples. Specifically, while far-UVC light has enough range to traverse microbes that are much smaller in size than human cells [less than 1 μm in diameter (*10, 11*), compared to the diameter of typical human cells ranging from about 10–25 μm (*10*)], it is strongly absorbed by the proteins in the cytoplasm of human cells (*12, 13*) and is drastically attenuated before reaching the human cell nucleus. It follows that far-UVC light is not able to penetrate the stratum corneum of skin and reach the underlying critical basal cells or melanocytes (*4*).

Another organ especially sensitive to UV damage is the lens; however, the lens is positioned distal to the cornea that is sufficiently thick [~500 μm (*14*))]. Therefore, penetration of far-UVC ~200-nm light through the cornea to the lens is predicted to be essentially zero (*15*).

The potential use of UVC light for microbe sterilization purposes in the presence of humans paves the way to numerous clinical applications, including reduction of surgical site infections (SSI) that are the second most common healthcare-associated infections resulting in readmissions, prolonged hospital stays, increased morbidity and mortality, and an overall higher medical cost (*16, 17*). A key factor contributing to the severity of SSI is the incidence of drug-resistant bacteria such as methicillin-resistant *Staphylococcus aureus* (MRSA) (*18, 19*).

To address the issue of reducing SSI, we have developed an approach that involves the use of inexpensive excimer lamps that, appropriately filtered, emit monoenergetic wavelengths in the far-UVC range. A crucial property of

[1] Address for correspondence: Center for Radiological Research, Columbia University Medical Center, 630 West 168th St., New York, NY 10032; email: djb3@cumc.columbia.edu.

UVC-mediated germicidal killing is that it is essentially independent of acquired drug resistance (*20, 21*).

We have previously shown that 207-nm light emitted by a filtered krypton-bromine (Kr-Br) excilamp has bactericidal efficacy while being minimally cytotoxic to human cells in a 3D skin tissue model *in vitro* (*7*) and in a hairless mouse skin model *in vivo* (*8*). Thus, continuous exposure of the wound to far-UVC light during surgery may inactivate the microbes alighting directly onto the surgical wound from the air. If proven to be safe to eyes as well as skin, continuous operation of far-UVC light would not require the use of cumbersome protective clothing, hoods and eye shields for the surgical staff and the patient (*22, 23*).

Here we extended those studies to a filtered krypton-chlorine (Kr-Cl) excimer lamp that produces essentially monoenergetic UV light at 222 nm and established that a wavelength window exist in the far-UVC region (from 200–222 nm) that inactivates bacteria efficiently but is not cytotoxic or mutagenic to mammalian cells.

We describe measurements of MRSA survival and of typical UV-induced premutagenic DNA lesions in a 3D human skin model immediately after exposure to different fluences of 222-nm light. We compared the results to those measured in samples exposed to similar fluences from a typical germicidal lamp emitting at 254 nm.

We further tested eight cellular and molecular endpoints relevant to skin damage *in vivo* in dorsal skin of hairless mice 48 h after exposure to 222-nm or 254-nm light used as positive control (*8*), at a fluence at which the 254-nm light is predicted to produce a significant decrease in SSI rates (*22*).

In agreement with our previous results using 207-nm light (*7, 8*), here we showed that 222-nm light has similar antimicrobial properties as a conventional germicidal lamp but without causing mammalian skin damage.

The finding that a far-UVC wavelength window (200–225 nm) is differentially cytotoxic to bacteria relative to mammalian cells is novel and can be used for various applications that would require the presence of humans, including room sterilization and reduction of surgical site infections, without the need of additional personal protective equipment.

MATERIALS AND METHODS

UV Lamps

We used an excimer lamp based on a krypton-chlorine (Kr-Cl) gas mixture that emits principally at 222 nm. The lamp (High Current Electronics Institute, Tomsk, Russia) was air cooled with a 6,000-mm^2 exit window (*24*). A custom bandpass filter (Omega Optical, Brattleboro, VT) was used to remove essentially all but the dominant 222-nm wavelength emission.

A UV spectrometer (Photon Control, BC, Canada) sensitive in the wavelength range from 200–360 nm was used to characterize the wavelength spectra emitted by the excimer lamp, and a deuterium lamp standard with a NIST-traceable spectral irradiance (Newport Corp, Stratford, CT) was used to calibrate the UV spectrometer.

Studies were also carried out with a conventional mercury germicidal lamp (Hygeaire, Atlantic Ultraviolet Corporation, Hauppauge, NY) with peak emission at 254 nm and used as positive control. An ILT1400 sensor equipped with a SEL220 detector (International Light Technologies, Peabody, MA) was used to measure the fluence rate from both lamps. For acute exposures (MRSA and 3D tissues), the 222- and 254-nm lamps were positioned 9 and 99 cm, respectively, from the sample at which corresponded a power density of 0.036 mJ/cm^2. For chronic exposures of mice, delivery of 157 mJ/cm^2 in a 7 h period was obtained by locating the 222- and the 254-nm lamps 41 and 205 cm from the samples, respectively; the corresponding power densities were 0.0062 mJ/cm^2 for the 222-nm lamp and 0.0008 mJ/cm^2 in the case of the conventional germicidal lamp.

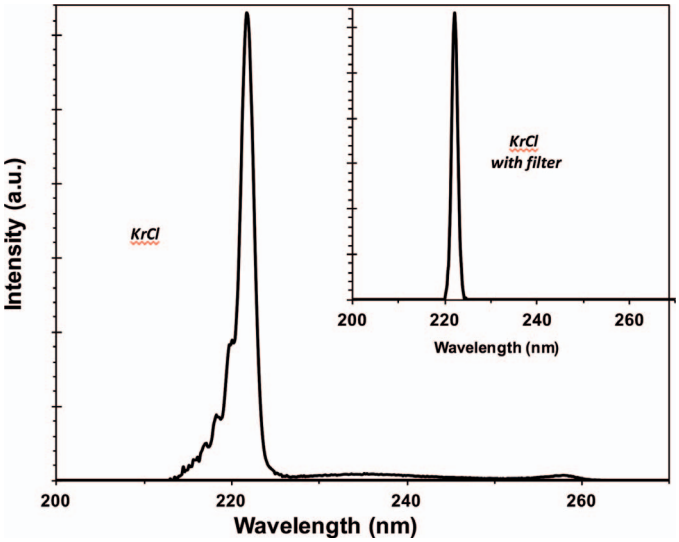

FIG. 1. Nonfiltered and filtered measured emission spectra from a Kr-Cl excimer lamp (main peak 222 nm).

Figure 1 shows the measured spectra emitted from the Kr-Cl excimer lamp that, together with the main excimer emission at 222 nm, also includes lower fluences of higher wavelength light (i.e. ~237 and ~258 nm). To remove these more penetrating higher wavelengths and therefore potentially more harmful to human cells, we used a custom bandpass filter (Omega Optical, Brattleboro, VT). As shown in the inset in Fig. 1, the filtered lamp effectively emitted only the characteristic single wavelength of 222 nm.

IN VITRO STUDIES

MRSA Cell Survival

We used methicillin-resistant *S. aureus* (MRSA USA300, multilocus sequence type 8, clonal complex 8, staphylococcal cassette chromosome *mec* type IV), which is a major cause of both community and nosocomial infections (*25–27*). Survival of MRSA as a function of UVC fluence was assessed immediately after exposure with the standard colony forming unit (CFU) assay, as previously reported (*7*).

UV-Associated Premutagenic DNA Lesions in a 3D Human Skin Model

We used a 3D human skin model EpiDerm-FT (MatTek Corp., Ashland, MA) consisting of stratum corneum and 8–12 human cell layers to reproduce human epidermis and dermis (*28*). We measured induction of the two most abundant premutagenic DNA lesions in the epidermis,

cyclobutane pyrimidine dimers (CPD) and pyrimidine-pyrimidone 6-4 photoproducts (6-4PP) (*4*), as a function of UVC fluence in 3D human skin constructs immediately after exposure using the immunohistochemical approach previously described (*7*).

IN VIVO STUDIES

Mouse Irradiations

We used six- to eight-week-old male hairless mice (SKH1-Elite strain 477, Charles River Laboratories, Stone Ridge, NY); the strain has UV action spectra for histological, physical and visible changes similar to those of human skin (*29, 30*). Moreover, the typical thickness of the stratum corneum of SKH1 mice (5–10 μm) (*31, 32*) is comparable to that of human skin (5–20 μm) (*33*).

One group of three mice was exposed to fluence of 157 mJ/cm^2 from 222 nm light delivered in a 7 h period by a filtered Kr-Cl excimer lamp while another group of three mice was sham irradiated to zero UV fluence. Mice exposed to 157 mJ/cm^2 delivered in 7 h period from 254 nm light represented the positive controls (*8*).

All animal procedures were carried out in accordance with federal guidelines and protocols approved by the Columbia University Medical Center IACUC.

Mouse Skin Safety-Specific Endpoints

Following the same protocols described in our previous mouse skin safety study (*8*), 48 h after UV exposure we measured the following endpoints: 1. Epidermal thickness measured in hematoxylin and eosin stained samples; 2. The percentage of proliferating keratinocytes expressing the Ki-67 antigen (*34, 35*). 3. Yields of UV-induced cyclobutane pyrimidine dimers (CPD) and 6-4 photoproducts (6-4PP); 4. The number of neutrophils and mast cells as markers of skin inflammation (*36*); 5. The expression of keratin (K) K6A as marker of skin differentiation (*37, 38*).

Tissues were examined with an Olympus IX70 microscope equipped with a Photometrics® PVCAM high-resolution, high-efficiency digital camera; Image-Pro Plus 6.0 software and Fiji/Image J software were used to analyze the images. For each mouse, each endpoint was measured in at least six randomly selected fields of view.

Statistical Analysis

Comparisons of mean values between treatment groups and controls were performed using Student's *t* test, and comparison of proportions were assessed with standard χ^2 tests.

IN VITRO RESULTS

MRSA Survival

We measured MRSA survival immediately after exposure to different fluences of 222-nm light generated by a filtered Kr-Cl excimer lamp (Fig. 2). We compared the results to survival of MRSA exposed to similar fluences from a conventional germicidal UV lamp (254 nm) (*7*). As illustrated in Fig. 2, at relatively high fluences at which the 254-nm light is predicted to produce a significant decrease in SSI rates (*1*), 222-nm light kills MRSA almost as efficiently as a conventional germicidal UV lamp. However, 254-nm light is almost equally efficient at killing human cells (*7*).

Induction of Premutagenic DNA Lesions in Human Skin

Figure 3 shows the comparison of the induced yields of CPD (left panel) and 6-4PP (right panel) in 3D skin tissue models exposed to 222-nm or 254-nm light. Unlike conventional germicidal light (254 nm), exposure to the 222-nm light at any of the studied fluences did not induce yields of either lesions that was significantly higher than the sham-irradiated samples.

IN VIVO RESULTS

Epidermal Thickness and Keratinocyte Proliferation

At 48 h after exposure, fixed dorsal skin sections were stained with hematoxylin and eosin (H&E) for analysis of epidermal thickness (Fig. 4A). As shown by the typical H&E-stained cross-sections of dorsal skin of sham-exposed mice (top panel), of mice exposed to 157 mJ/cm^2 from 254-nm light (middle panel) or 222-nm light (bottom panel), we found that, unlike the 254-nm light, the epidermal thickness of skin of mice exposed to the 222-nm excimer lamp was not statistically different from skin of unexposed mice ($P = 0.18$) (Fig. 4B and Table 1).

Figure 4C shows representative cross-sectional images of skin samples comparing Ki-67 expression in sham-exposed mice (Fig. 4A, top panel), in skin of mice exposed to 157 mJ/cm^2 from 254-nm light (Fig. 4A, middle panel) or 222-nm light (Fig. 4A, bottom panel). We found that Ki-67 expression in keratinocytes of skin exposed to the 222-nm excimer lamp was not statistically different from control ($P = 0.52$) (Fig. 4D and Table 1). In contrast, the same fluence from the 254-nm germicidal lamp triggered keratinocytes hyper-proliferation (Ki-67 expression increased by 2.5-fold compared to controls, $P < 0.0001$) (Fig. 4D and Table 1); this was consistent with severe tissue hyperplasia induced by 254-nm light as measured by a ~3-fold increase in epidermal thickness ($P < 0.0001$) (Fig. 4B and Table 1).

Premutagenic UV-Associated DNA Lesions

Figure 5A shows representative cross-sectional images of sham-irradiated mice or skin of mice exposed to 157 mJ/cm^2 from 222-nm light or 254-nm light, comparing premutagenic skin lesions CPD (Fig. 5A, top panels) and 6-4PP (Fig. 5A, bottom panels). In agreement with our

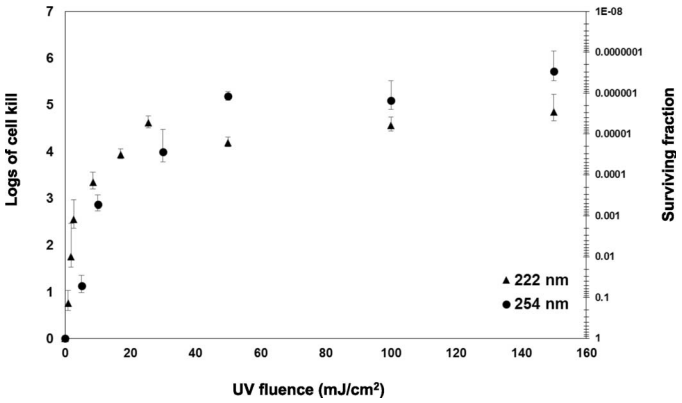

FIG. 2. Bacterial cell killing induced by 222- and 254-nm UV light. Killing of MRSA (strain USA300) is shown relative to zero-fluence controls, expressed as surviving fraction or as logs of cell kill (–log10[surviving fraction]), produced by different fluences of UV light from a filtered 222-nm Kr-Cl excimer lamp (▲) or a germicidal 254-nm lamp (●).

previous findings (*7, 8*), we measured no increase in UV-induced DNA photodamage in 222-nm exposed skin relative to controls ($P = 0.18$ for CPD and $P = 0.41$ for 6-4PP). On the contrary, exposure to the same fluence from a conventional germicidal lamp (254 nm) caused a dramatic increase of both lesions relative to respective controls ($P < 0.0001$) (Fig. 5B and C, respectively, and Table 1).

Skin Inflammation

To assess UV-induced cell inflammation, we measured the density of the markers mast cells and neutrophyls [i.e., myeloperoxidase (MPO)-positive cells] (Fig. 6). Although 254-nm light caused a statistically significant increase of both markers ($P < 0.0005$) (Fig. 6 and Table 1), the density of mast cells and neutrophyls induced by the 222-nm light (Fig. 6A and B, respectively) was not statistically distinguishable from controls ($P = 0.68$ and $P = 0.59$, respectively).

Skin Differentiation

We measured keratinocyte differentiation as keratin (K) 6A expression in skin of mice exposed to 222-nm light and compared the results to K6A expression in sham-exposed mice and in mice exposed to 254-nm light used as positive control. Figure 7 illustrates typical cross-sectional images of sham-exposed mice (Fig. 7, top panel), skin of mice exposed to 157 mJ/cm^2 from 254-nm light (Fig. 7, middle panel) or from 222-nm light (Fig. 7, bottom panel). The expression level of K6A in 222-nm exposed skin was not statistically different from controls ($P = 0.22$) (Table 1). This is in contrast with a ~3-fold increase of newly synthesized K6A in samples exposed to light from a conventional germicidal lamp ($P < 0.0001$).

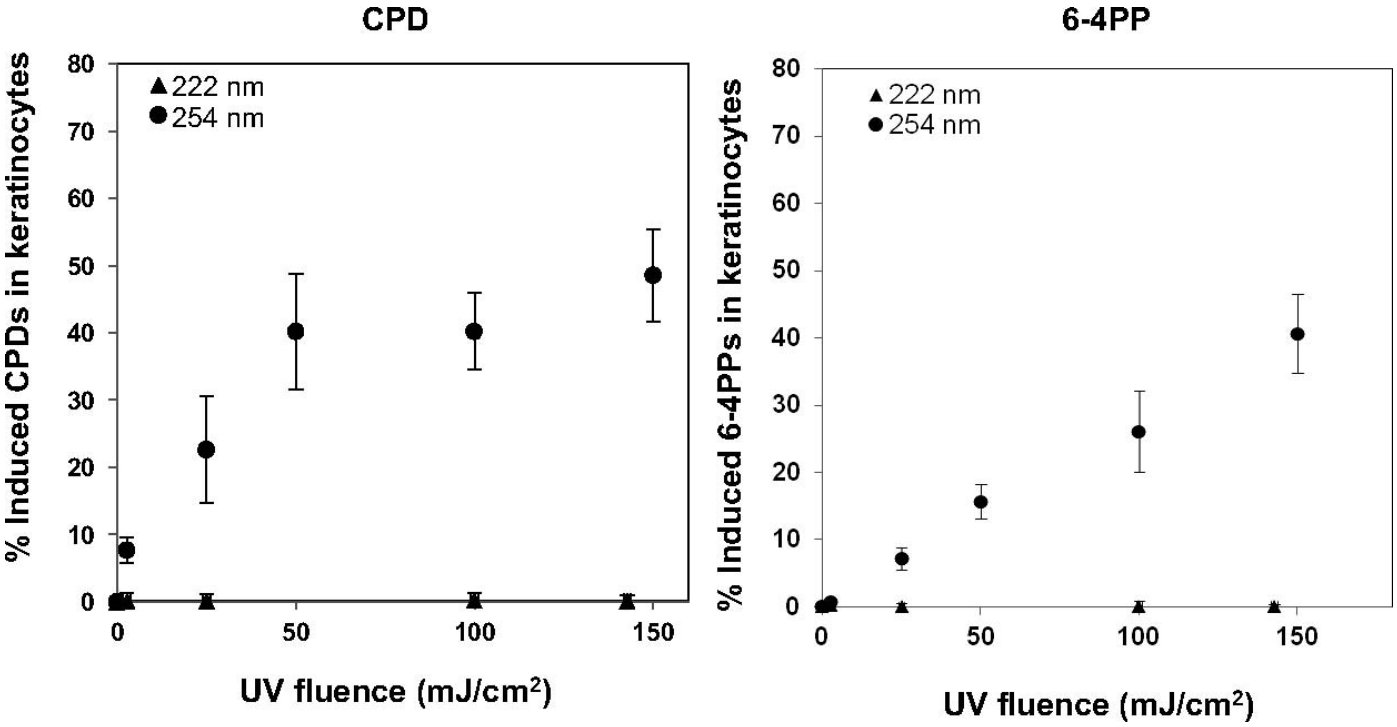

FIG. 3. Premutagenic skin DNA lesion yields induced by 222- and 254-nm UV light. Yields of cyclobutane pyrimidine dimers (CPD) (left panel) and pyrimidine-pyrimidone 6-4 photoproducts (6-4PP) (right panel) in keratinocytes in a 3D human skin tissue model, induced by conventional germicidal UV radiation (●) and by 222-nm UV light (▲). In both graphs zero-fluence control measurements (<1%) have been subtracted from the data.

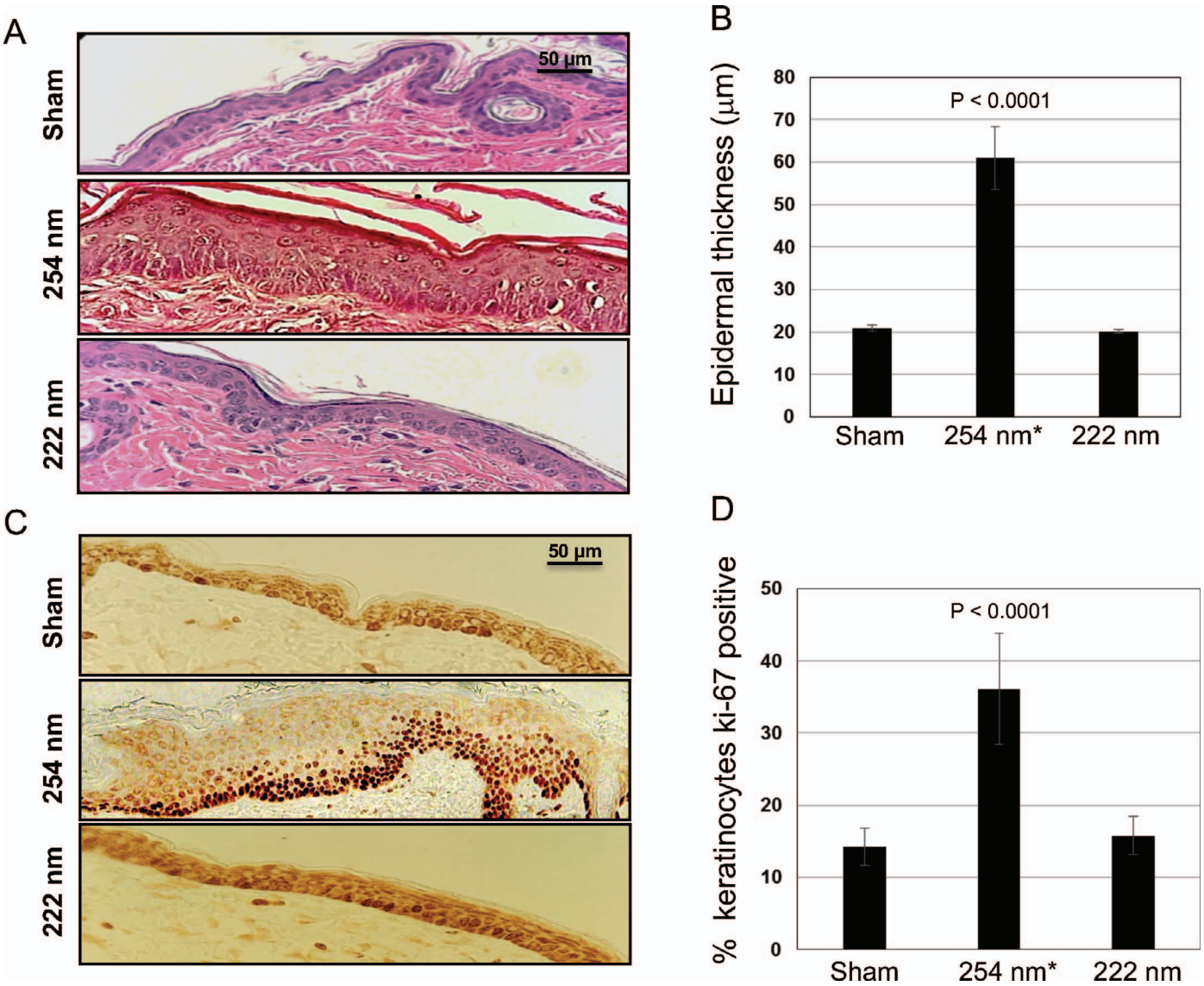

FIG. 4. Epidermal thickness and keratinocyte proliferation in mouse skin exposed to UVC light. Panel A: Representative cross-sectional images of H&E-stained mouse dorsal skin comparing the epidermal thickness in sham-exposed mice (top panel), in mice exposed to 157 mJ/cm^2 from 254-nm light (middle panel) or from 222-nm light (bottom panel). Panel B: Quantification of epidermal thickness. Panel C: Ki-67-positive keratinocytes (dark brown-stained cells) in typical cross-sections of skin of sham-exposed mice (top panel), of mice exposed to 254-nm light (middle panel) or to 222-nm light (bottom panel). Panel D: Quantification of the percentage of keratinocytes expressing Ki-67 antigen. Values represent the average ± SD of epidermal thickness measured in nine randomly selected fields of view per mouse (n = 3). *Values from elsewhere (*8*).

TABLE 1
Summary of the Combined Results for Each Endpoint

Endpoint	Controls	222 nm	222 nm *P* value	254 nm*	254 nm *P* value
Epidermal thickness (µm)	21.0 ± 0.8	20.1 ± 0.4	0.18	60.9 ± 7.4	<0.0001
Ki-67 positive keratinocytes (%)	14.2 ± 2.6	15.8 ± 2.7	0.52	36.1 ± 7.7	<0.0001
CPD positive keratinocytes (%)	0.43 ± 0.01	0.47 ± 0.03	0.18	52.3 ± 5.6	<0.0001
6-4PP positive keratinocytes (%)	0.50 ± 0.06	0.45 ± 0.03	0.41	31.1 ± 1.4	<0.0001
Density of mast cells (number/cm^2)	28.5 ± 11.9	30.6 ± 14.2	0.68	86.6 ± 16.8	<0.0005
Density of MPO positive cells (number/cm^2)	24.2 ± 9.1	27.2 ± 5.7	0.59	202.4 ± 11.3	<0.0005
K6A optical density (%)	15.9 ± 5.7	18.9 ± 6.7	0.22	45.8 ± 6.9	<0.0001

* Values from elsewhere (*8*).

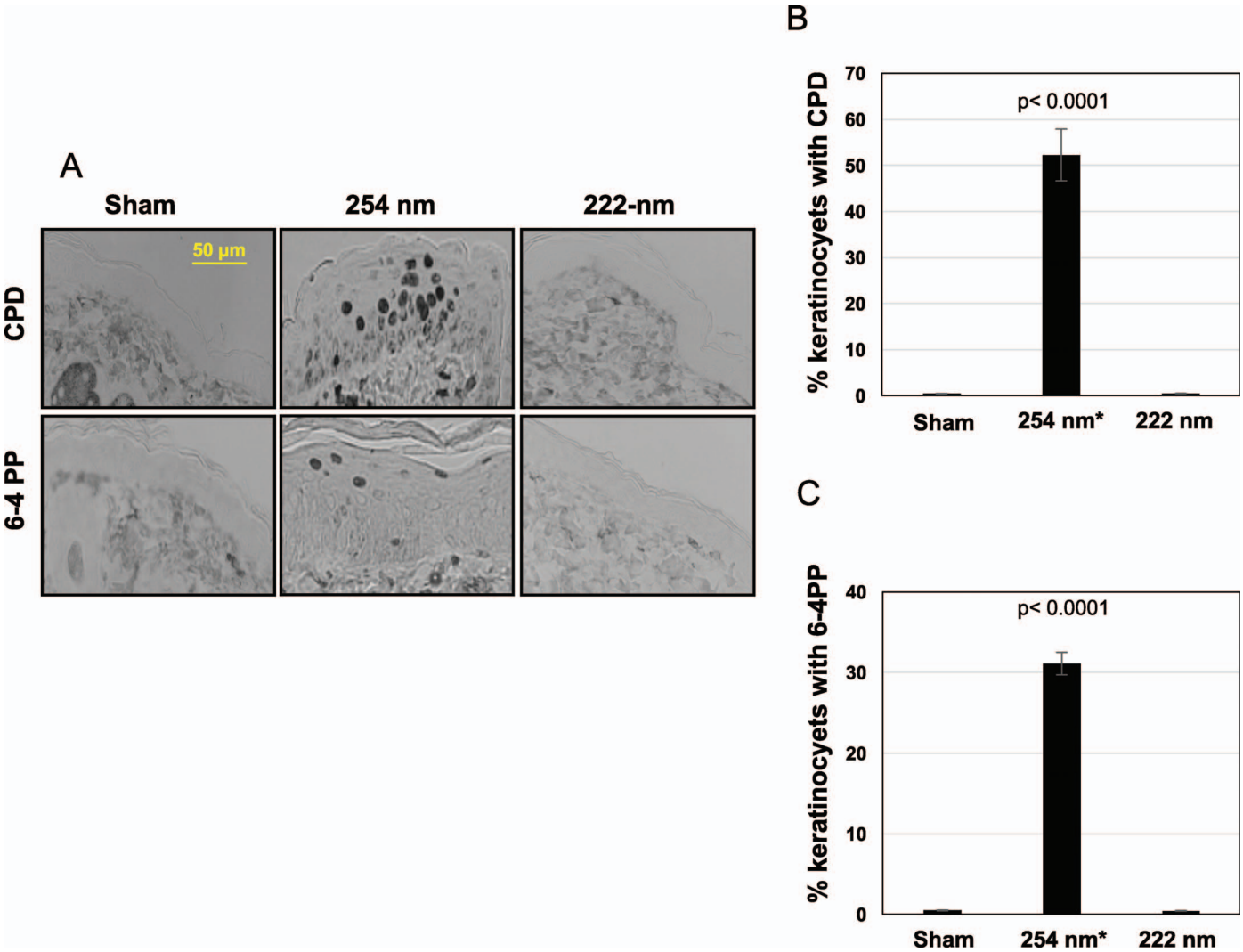

FIG. 5. UVC-induced premutagenic DNA lesions in mouse skin. Panel A: Representative cross-sectional images of dorsal skin samples comparing premutagenic skin lesions CPD (top row, dark-stained cells) and 6-4PP (bottom row, dark-stained cells) in the epidermis of sham-exposed mice (left column), of mice exposed to 157 mJ/cm^2 from 254-nm light (middle column) or 222-nm light (right column). Quantification of the percentage of keratinocytes showing (panel B) CPD and (panel C) 6-4PP dimers. Values represent the average ±SD of cells exhibiting dimers measured in nine randomly selected fields of view per mouse (n = 3). *Value from elsewhere (*8*).

DISCUSSION

Here we showed that 222 nm is essentially equi-effective at killing antibiotic-resistant bacteria as conventional germicidal UV lamps (254 nm). However, compared to the latter, 222-nm light does not induce typical UV-associated premutagenic DNA lesions in human keratinocytes in a 3D human skin model and appears to be safe for skin of exposed hairless mice, as assessed by eight cellular and molecular endpoints associated with damaged skin.

The results are consistent with previous *in vitro* and *in vivo* findings using a filtered krypton-bromine lamp that emits light at 207 nm (*7, 8*); this suggests that there is a range of wavelengths, specifically between 200 and 222 nm, which are equitoxic to bacteria as typical germicidal lamps emitting at 254 nm, but without associated skin damage risks.

The lack of induced damage is due to the limited penetration of far-UVC light in biological samples (*39*): while light in the 200-222 nm region can traverse microbes that are much smaller in size (<1 µm) (*10, 11, 40*) than a typical mammalian cell (~10–25 µm in diameter) (*10*), it cannot penetrate mammalian cells cytoplasm (*7*) as well as all tissues with a stratum corneum (*8*).

A central application of our approach is reduction of SSI, which still represent a major complication of surgical procedures (*41*). Current evidence suggests that the majority of SSI result from bacteria alighting directly onto the surgical wound from the air (*22, 42–44*). Based on our previous studies (*7, 8*) and on the preclinical results reported here, lamps emitting far-UVC light in the 200–222 nm range could potentially be used for continuous low-fluence/low-rate exposures during the course of a surgical procedure to inactivate bacteria before they penetrate into the interior

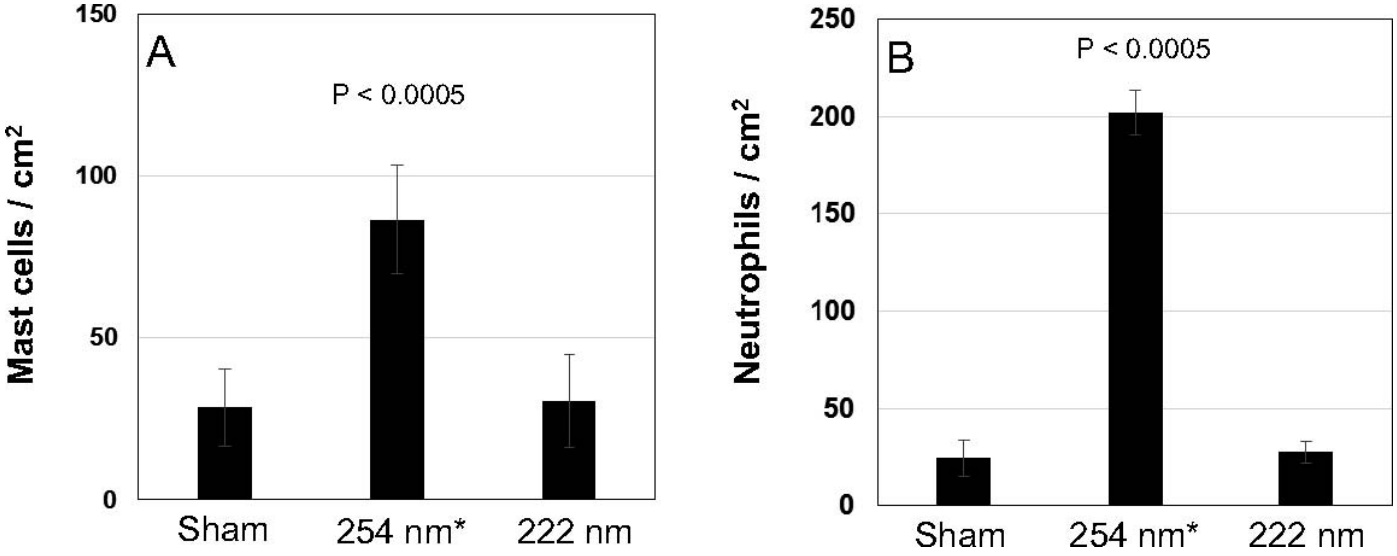

FIG. 6. UVC-induced inflammation in mouse skin. Density of (panel A) mast cells and (panel B) cells expressing the myeloperoxidase (MPO) enzyme (i.e., neutrophils) in the epidermis of sham-exposed mice, of mice exposed to 157 mJ/cm^2 from 254-nm light or 222-nm light. Values represent the average ±SD of the number of cells/m^2 measured in six randomly selected fields of view per mouse (n = 3). *Value from elsewhere (*8*).

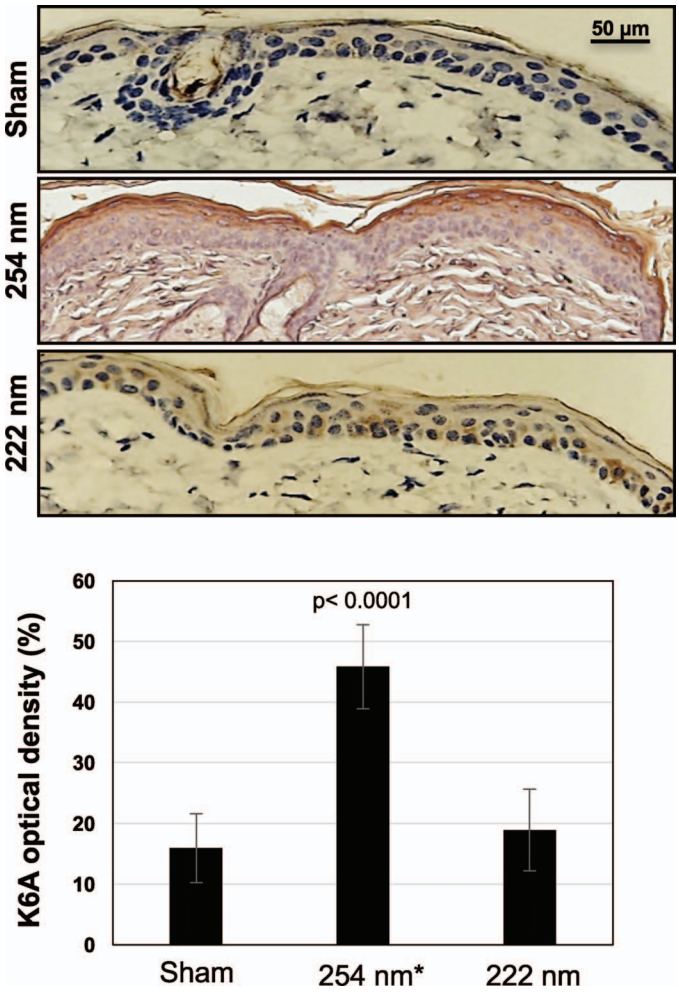

FIG. 7. Tissue differentiation in UVC-exposed mouse skin. Representative cross-sectional images of mouse dorsal epidermis expressing K6A (brown stained area) with relative quantification. Mice were sham exposed (top panel), exposed to 157 mJ/cm^2 from 254-nm light (middle panel) or 222-nm light (bottom panel). Values represent the average ± SD of the percentage of keratin optical density measured in nine randomly selected fields of view per mouse (n = 3). *Value from elsewhere (*8*).

of the wound. At bactericidal fluences, far-UVC light cannot traverse tissues with a stratum corneum such as skin and lens of the eyes. The use of this light would therefore not require additional protective clothing for patients or medical staff and could become a standard in hospital environments to reduce SSI rates, particularly those due to drug-resistant pathogens. In addition, targeting bacteria as they alight onto the wound would prevent the formation of bacterial clusters or biofilms (*45*), which are difficult to eradicate and impede wound healing (*46*).

Other potential applications of far-UVC light is sterilization of any environment with a high likelihood of airborne-based pathogen transmission, including tuberculosis, small pox, severe acute respiratory syndrome (SARS) and pandemic influenza, which collectively affects one billion people annually (*47*). Although upper-room UV-irradiation systems based on conventional broad-spectrum UV lamps (*48*) have long been considered for room sterilization (*49–51*), they cannot be widely used due to safety concerns relating to skin cancer and cataract risks (*49, 52, 53*).

Collectively, our studies suggest that far-UVC light (200–225 nm), unlike conventional UV germicidal lamps, has considerable promise to be a safe and inexpensive modality for SSI reduction, while being cytotoxic to both drug-resistant and drug-sensitive microbes (*22*).

ACKNOWLEDGMENTS

We are very grateful to Lynn Shostack for her support and advice. We thank Ms. Elizabeth Flores of the Department of Medicine and Infectious Disease at Columbia University for her expertise and for the use of the laboratory equipment. We thank Drs. Alan W. Bigelow and Yanping Xu for their insight in the UV dosimetry. GR-P receives royalty payments from Ushio Inc. (Tokyo, Japan) pursuant to exclusive license and research agreements with Columbia University.

Accepted: January 15, 2017; published online: February 22, 2017

REFERENCES

1. Yin R, Dai T, Avci P, Jorge AE, de Melo WC, Vecchio D, et al. Light based anti-infectives: ultraviolet C irradiation, photodynamic therapy, blue light, and beyond. Curr Opin Pharmacol 2013; 13(5): 731–62.
2. McDevitt JJ, Rudnick SN, Radonovich LJ. Aerosol Susceptibility of Influenza Virus to UV-C Light. Appl Environ Microbiol 2012; 78(6):1666–9.
3. Mitchell DL, Nairn RS. The (6-4) photoproduct and human skin cancer. Photo-dermatol 1988; 5(2):61–4.
4. Pfeifer GP, Besaratinia A. UV wavelength-dependent DNA damage and human non-melanoma and melanoma skin cancer. Photochem Photobiol Sci 2012; 11(1):90–7.
5. Jose JG, Pitts DG. Wavelength dependency of cataracts in albino mice following chronic exposure. Exp Eye Res 1985; 41(4): 545–63.
6. Soderberg PG. Acute cataract in the rat after exposure to radiation in the 300 nm wavelength region. A study of the macro-, micro- and ultrastructure. Acta Ophthalmol 1988; 66(2):141–52.
7. Buonanno M, Randers-Pehrson G, Bigelow AW, Trivedi S, Lowy FD, Spotnitz HM, et al. 207-nm UV light - A promising tool for safe low-cost reduction of surgical site infections. I: In vitro studies. PLoS ONE, DOI: 101371/journalpone0076968. eCollection 2013.
8. Buonanno M, Stanislauskas M, Ponnaiya B, Bigelow AW, Randers-Pehrson G, Shuryak I, et al. 207-nm UV light - A promising tool for safe low-cost reduction of surgical site infections. II: In-vivo safety studies. PLoS One. 2016 Jun 8; 11(6):e0138418. doi: 10.1371/journal.pone.0138418. PMID: 27275949
9. Sosnin EA, Oppenlander T, Tarasenko VF. Applications of capacitive and barrier discharge excilamps in photoscience. J Photochem Photobiol C: Photochem Rev 2006; 7:145–63.
10. Metzler DE, Metzler CM. Biochemistry: The Chemical Reactions of Living Cells. 2nd ed. San Diego: Academic Press; 2001.
11. Lorian V, Zak O, Suter J, Bruecher C. Staphylococci, in vitro and in vivo. Diagn Microbiol Infect Dis1985; 3(5):433–44.
12. Goldfarb AR, Saidel LJ. Ultraviolet absorption spectra of proteins. Science 1951; 114(2954):156–7.
13. Setlow J. The molecular basis of biological effects of ultraviolet radiation and photoreactivation. In: Ebert M, Howard A, editors. Current topics in radiation research. II. Amsterdam: North Holland Publishing Company; 1966. p. 195–248.
14. Doughty MJ, Zaman ML. Human corneal thickness and its impact on intraocular pressure measures: a review and meta-analysis approach. Surv Ophthalmol 2000; 44(5):367–408.
15. Kolozsvari L, Nogradi A, Hopp B, Bor Z. UV absorbance of the human cornea in the 240- to 400-nm range. Invest Ophthalmol Vis Sci 2002; 43(7):2165–8.
16. Anderson DJ. Surgical site infections. Infect Dis Clin North Am 2011; 25(1):135–53.
17. Allegranzi B, Bischoff P, de Jonge S, Kubilay NZ, Zayed B, Gomes SM, et al. New WHO recommendations on preoperative measures for surgical site infection prevention: an evidence-based global perspective. Lancet Infect Dis 2016.
18. Fry DE, Barie PS. The changing face of Staphylococcus aureus: a continuing surgical challenge. Surg Infect 2011; 12(3):191–203.
19. Anderson DJ, Kaye KS. Staphylococcal surgical site infections. Infect Dis Clin North Am. 2009; 23(1):53–72.
20. Conner-Kerr TA, Sullivan PK, Gaillard J, Franklin ME, Jones RM. The effects of ultraviolet radiation on antibiotic-resistant bacteria in vitro. Ostomy Wound Manage 1998; 44(10):50–6.
21. Rao BK, Kumar P, Rao S, Gurung B. Bactericidal effect of ultraviolet C (UVC), direct and filtered through transparent plastic, on gram-positive cocci: an in vitro study. Ostomy Wound Manage 2011; 57(7):46–52.
22. Ritter MA, Olberding EM, Malinzak RA. Ultraviolet lighting during orthopaedic surgery and the rate of infection. J Bone Joint Surg Am 2007; 89(9):1935–40.
23. Berg M, Bergman BR, Hoborn J. Ultraviolet radiation compared to an ultra-clean air enclosure. Comparison of air bacteria counts in operating rooms. J Bone Joint Surg Br 1991; 73(5):811–5.
24. Sosnin EA, Avdeev SM, Kuznetzova EA, Lavrent'eva LV. A bacterial barrier-discharge KrBr Excilamp. Instr Experiment Tech 2005; 48:663–6.
25. Anderson DJ, Sexton DJ, Kanafani ZA, Auten G, Kaye KS. Severe surgical site infection in community hospitals: epidemiology, key procedures, and the changing prevalence of methicillin-resistant Staphylococcus aureus. Infect Control Hosp Epidemiol 2007; 28(9):1047–53.
26. Hidron AI, Edwards JR, Patel J, Horan TC, Sievert DM, Pollock DA, et al. NHSN annual update: antimicrobial-resistant pathogens associated with healthcare-associated infections: annual summary of data reported to the National Healthcare Safety Network at the Centers for Disease Control and Prevention, 2006-2007. Infect Control Hosp Epidemiol 2008; 29(11):996–1011.
27. Lessa FC, Mu Y, Ray SM, Dumyati G, Bulens S, Gorwitz RJ, et al. Impact of USA300 methicillin-resistant Staphylococcus aureus on clinical outcomes of patients with pneumonia or central line-associated bloodstream infections. Clin Infect Dis 2012; 55(2): 232–41.
28. Kubilus J, Hayden PJ, Ayehunie S, Lamore SD, Servattalab C, Bellavance KL, et al. Full thickness epiderm: a dermal-epidermal skin model to study epithelial-mesenchymal interactions. Altern Lab Anim 2004; 32 Suppl 1A:75-82.
29. Bissett DL, Hannon DP, Orr TV. Wavelength dependence of histological, physical, and visible changes in chronically UV-irradiated hairless mouse skin. Photochem Photobiol 1989; 50(6): 763–9.
30. Bissett DL, Hannon DP, Orr TV. An animal model of solar-aged skin: histological, physical, and visible changes in UV-irradiated hairless mouse skin. Photochem Photobiol 1987; 46(3):367–78.
31. Sato K, Sugibayashi K, Morimoto Y. Species differences in percutaneous absorption of nicorandil. J Pharm Sci 1991; 80(2): 104–7.
32. Bronaugh RL, Stewart RF, Congdon ER. Methods for in vitro percutaneous absorption studies. II. Animal models for human skin. Toxicol Appl Pharmacol 1982; 62(3):481–8.
33. Russell LM, Wiedersberg S, Delgado-Charro MB. The determination of stratum corneum thickness: an alternative approach. Eur J Pharm Biopharm 2008; 69(3):861–70.
34. van Diest PJ, Brugal G, Baak JP. Proliferation markers in tumours: interpretation and clinical value. J Clin Pathol 1998; 51(10): 716–24.
35. Scholzen T, Gerdes J. The Ki-67 protein: from the known and the unknown. J Cell Physiol. 2000; 182(3):311–22.
36. Terui T, Okuyama R, Tagami H. Molecular events occurring behind ultraviolet-induced skin inflammation. Curr Opin Allergy Clin Immunol 2001; 1(5):461–7.

37. Horio T, Miyauchi H, Sindhvananda J, Soh H, Kurokawa I, Asada Y. The effect of ultraviolet (UVB and PUVA) radiation on the expression of epidermal keratins. Br Dermatol 1993; 128(1):10–5.

38. Sano T, Kume T, Fujimura T, Kawada H, Higuchi K, Iwamura M, et al. Long-term alteration in the expression of keratins 6 and 16 in the epidermis of mice after chronic UVB exposure. Arch Dermatol Res 2009; 301(3):227–37.

39. Green H, Boll J, Parrish JA, Kochevar IE, Oseroff AR. Cytotoxicity and mutagenicity of low intensity, 248 and 193 nm excimer laser radiation in mammalian cells. Cancer Res 1987; 47(2):410–3.

40. Coohill TP. Virus-cell interactions as probes for vacuum-ultraviolet radiation damage and repair. Photochem Photobiol 1986; 44(3):359–63.

41. Crolla RM, van der Laan L, Veen EJ, Hendriks Y, van Schendel C, Kluytmans J. Reduction of surgical site infections after implementation of a bundle of care. PLoS One 2012; 7(9):e44599.

42. Lidwell OM, Lowbury EJ, Whyte W, Blowers R, Stanley SJ, Lowe D. Airborne contamination of wounds in joint replacement operations: the relationship to sepsis rates. J Hosp Infect 1983; 4(2):111–31.

43. Gosden PE, MacGowan AP, Bannister GC. Importance of air quality and related factors in the prevention of infection in orthopaedic implant surgery. J Hosp Infect 1998; 39(3):173–80.

44. Stocks GW, O'Connor DP, Self SD, Marcek GA, Thompson BL. Directed air flow to reduce airborne particulate and bacterial contamination in the surgical field during total hip arthroplasty. J Arthroplasty 2011; 26(5):771–6.

45. de Carvalho CC. Biofilms: recent developments on an old battle. Recent Pat Biotechnol 2007; 1(1):49–57.

46. Rahim K, Saleha S, Zhu X, Huo L, Basit A, Franco OL. Bacterial contribution in chronicity of wounds. Microb Ecol 2016.

47. Uplekar M, Weil D, Lonnroth K, Jaramillo E, Lienhardt C, Dias HM, et al. WHO's new end TB strategy. Lancet 2015; 385(9979): 1799–801.

48. Reed NG. The history of ultraviolet germicidal irradiation for air disinfection. Public Health Rep 2010; 125(1):15–27.

49. Nardell EA, Bucher SJ, Brickner PW, Wang C, Vincent RL, Becan-McBride K, et al. Safety of upper-room ultraviolet germicidal air disinfection for room occupants: results from the Tuberculosis Ultraviolet Shelter Study. Public Health Rep 2008; 123(1):52–60.

50. Escombe AR, Moore DA, Gilman RH, Navincopa M, Ticona E, Mitchell B, et al. Upper-room ultraviolet light and negative air ionization to prevent tuberculosis transmission. PLoS Med 2009; 6(3):e43.

51. Linnes JC, Rudnick SN, Hunt GM, McDevitt JJ, Nardell EA. Eggcrate UV: a whole ceiling upper-room ultraviolet germicidal irradiation system for air disinfection in occupied rooms. Indoor Air 2014; 24(2):116–24.

52. Wengraitis S, Reed NG. Ultraviolet spectral reflectance of ceiling tiles, and implications for the safe use of upper-room ultraviolet germicidal irradiation. Photochem Photobiol 2012; 88(6):1480–8.

53. Sliney D. Balancing the risk of eye irritation from UV-C with infection from bioaerosols. Photochem Photobiol 2013; 89(4): 770–6.